Cell Reports, Volume *22*

Supplemental Information

The Aging Astrocyte Transcriptome from Multiple Regions of the Mouse Brain

Matthew M. Boisvert, Galina A. Erikson, Maxim N. Shokhirev, and Nicola J. Allen

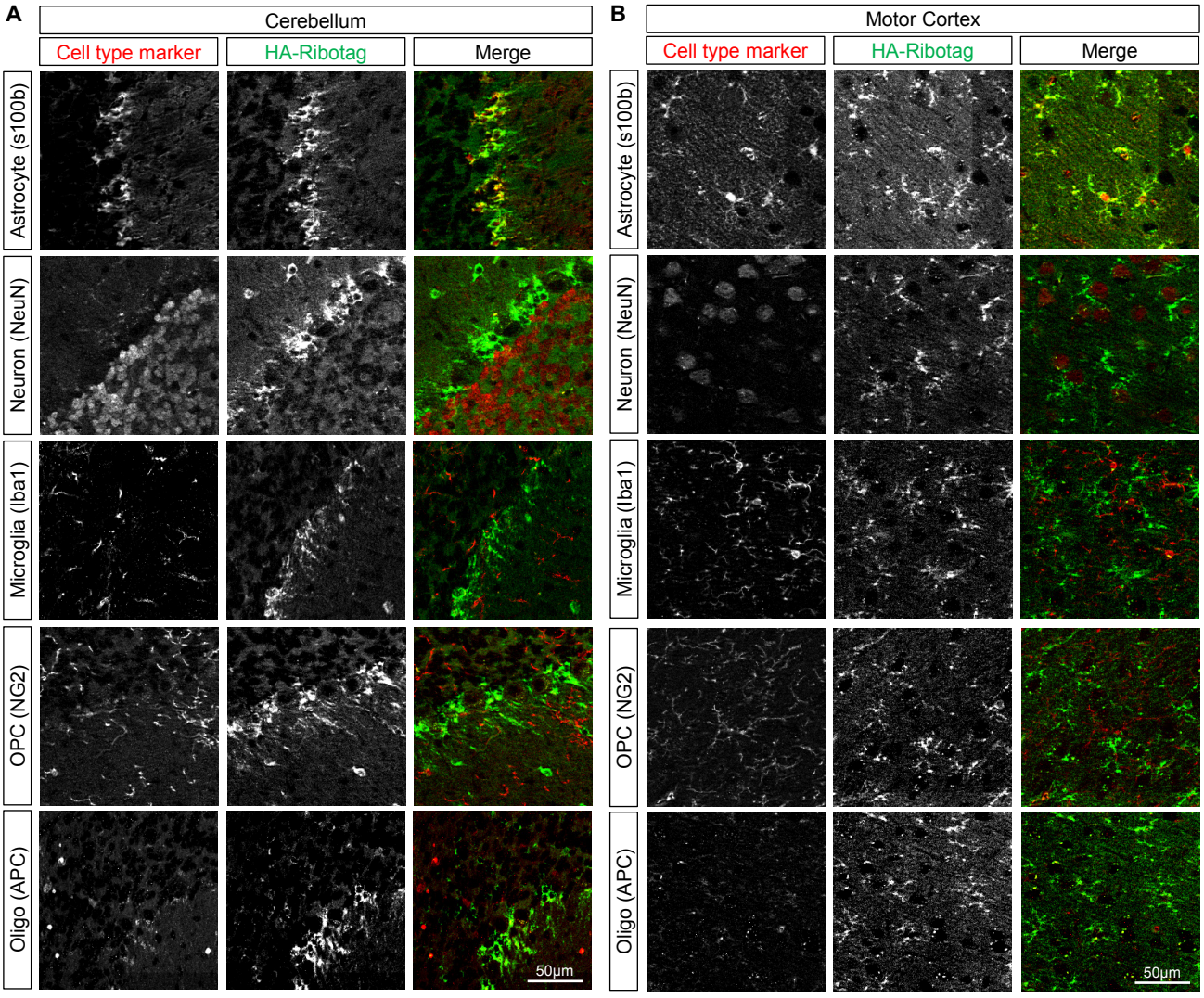

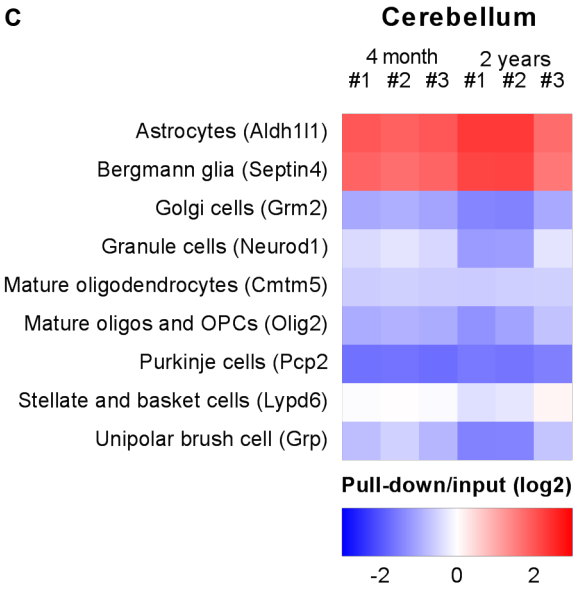

Figure S1, relates to Figure 1,2. Validation of astrocyte-ribotag model in the cerebellum and motor cortex. Immunostaining for HA and cell-specific markers, to determine cell-type expression of HA, in the cerebellum (**A**) and motor cortex (**B**). Images shown are cropped from a larger mosaic tiled image **C.** Analysis of cerebellum RNAseq data for cerebellar cell type-specific mRNA, comparing HA-tagged ribosome pulldown mRNA (astrocyte) to the total lysate mRNA (input sample), as in Fig 2, but with cerebellum specific gene lists developed from (Doyle et al., 2008). Cre line from which the pulldown in Doyle data was derived is labeled in parentheses.

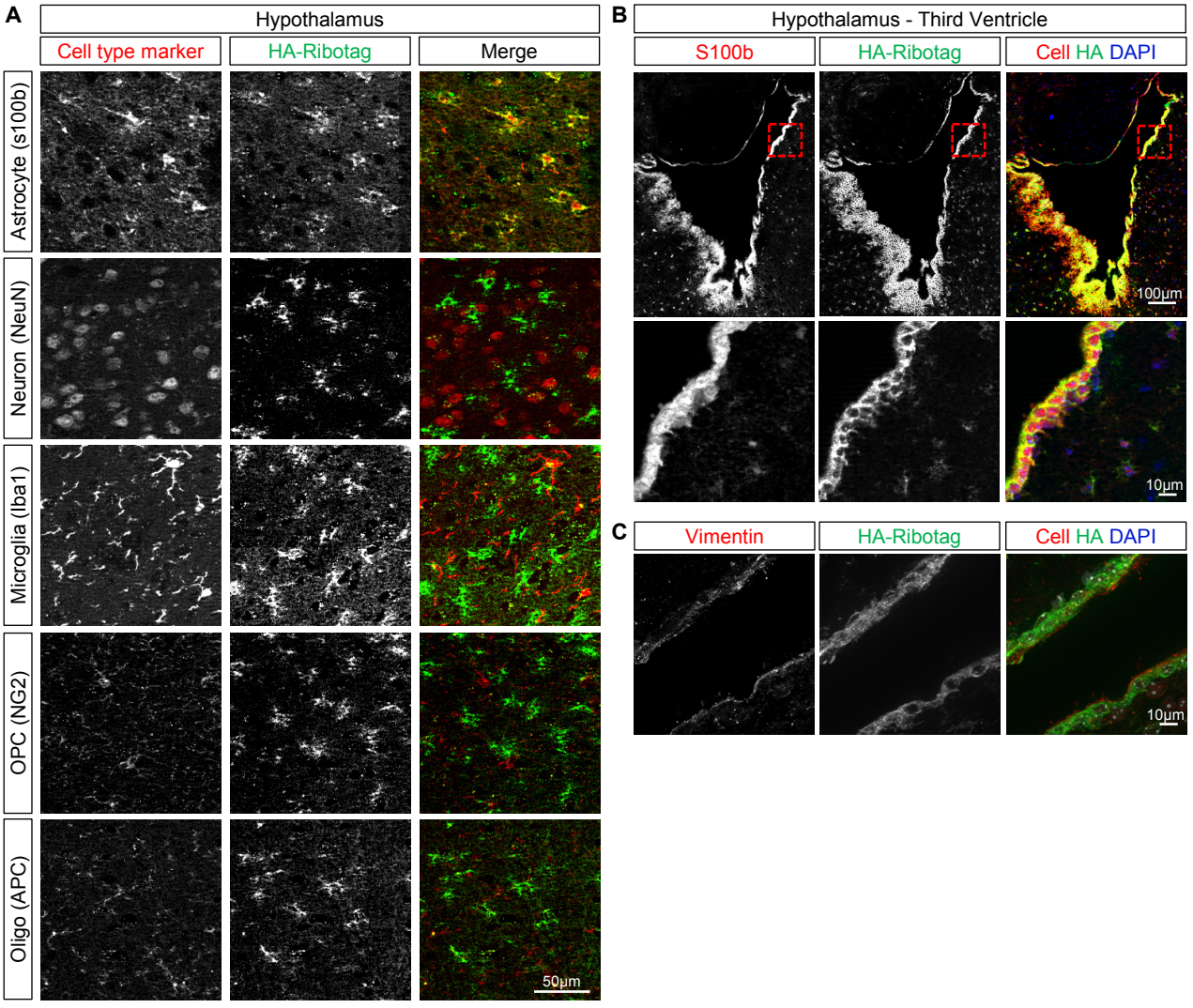

Figure S2, relates to Figure 1. Validation of astrocyte-ribotag model in the hypothalamus. Immunostaining for HA and cell-specific markers, to determine cell-type expression of HA in the hypothalamus (**A**). Images shown are cropped from a larger mosaic tiled image **B, C.** Immunostaining for HA and S100b (**B**) or vimentin (**C**) in the third ventricle of the hypothalamus, to detect expression of HA-tagged ribosomes in α-tanycyte/ependymal cells. Box indicates zoom area in **B.**

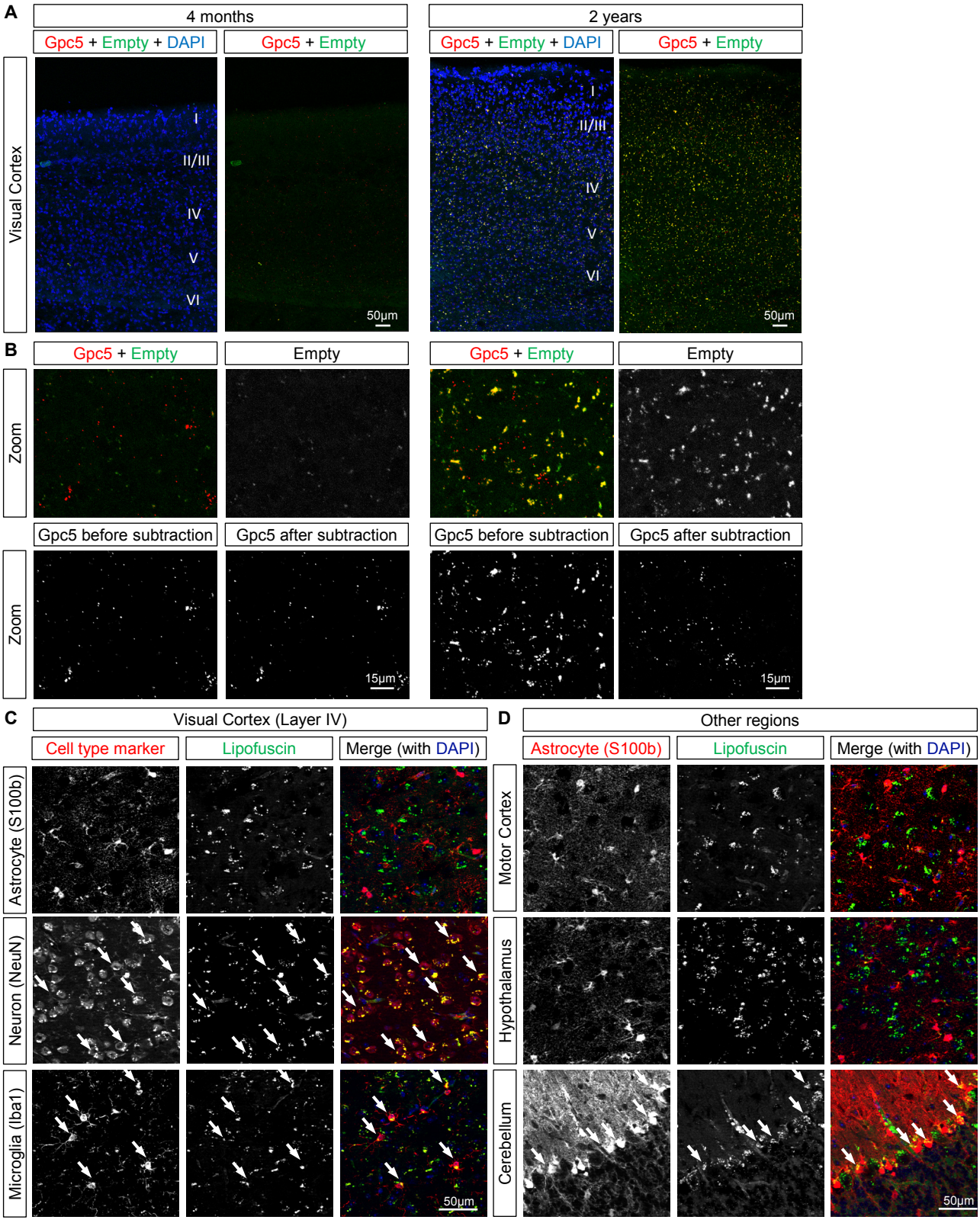

Figure S3, relates to Figure 3. Subtraction of lipofuscin background from *in situ* samples and lipofuscin cellular localization. A. Raw images of *in situ* hybridization of *Gpc5* in the visual cortex of 4 month (left) and 2 year old (right) mouse brain (note same example images as Fig S4). Images are mosaic image of tiles acquired at 20x **B.** Images of *Gpc5 in situ* on 4 month (left) and 2 year old (right) cortex with probe and empty (unlabeled channel, with autofluorescence indicative of lipofuscin) channels, alone and merged, with lower right panels showing the *Gpc5* channel after subtracting the "empty" channel. **C,D.** Immunostaining for cell-type markers and lipofuscin (autofluorescence) in 2 year old brain, in layer IV of visual cortex (**C**), and for astrocytes in the motor cortex, hypothalamus, and cerebellum (**D**), with arrows marking example cell-lipofuscin overlap. Images shown are cropped from a larger mosaic tiled image.

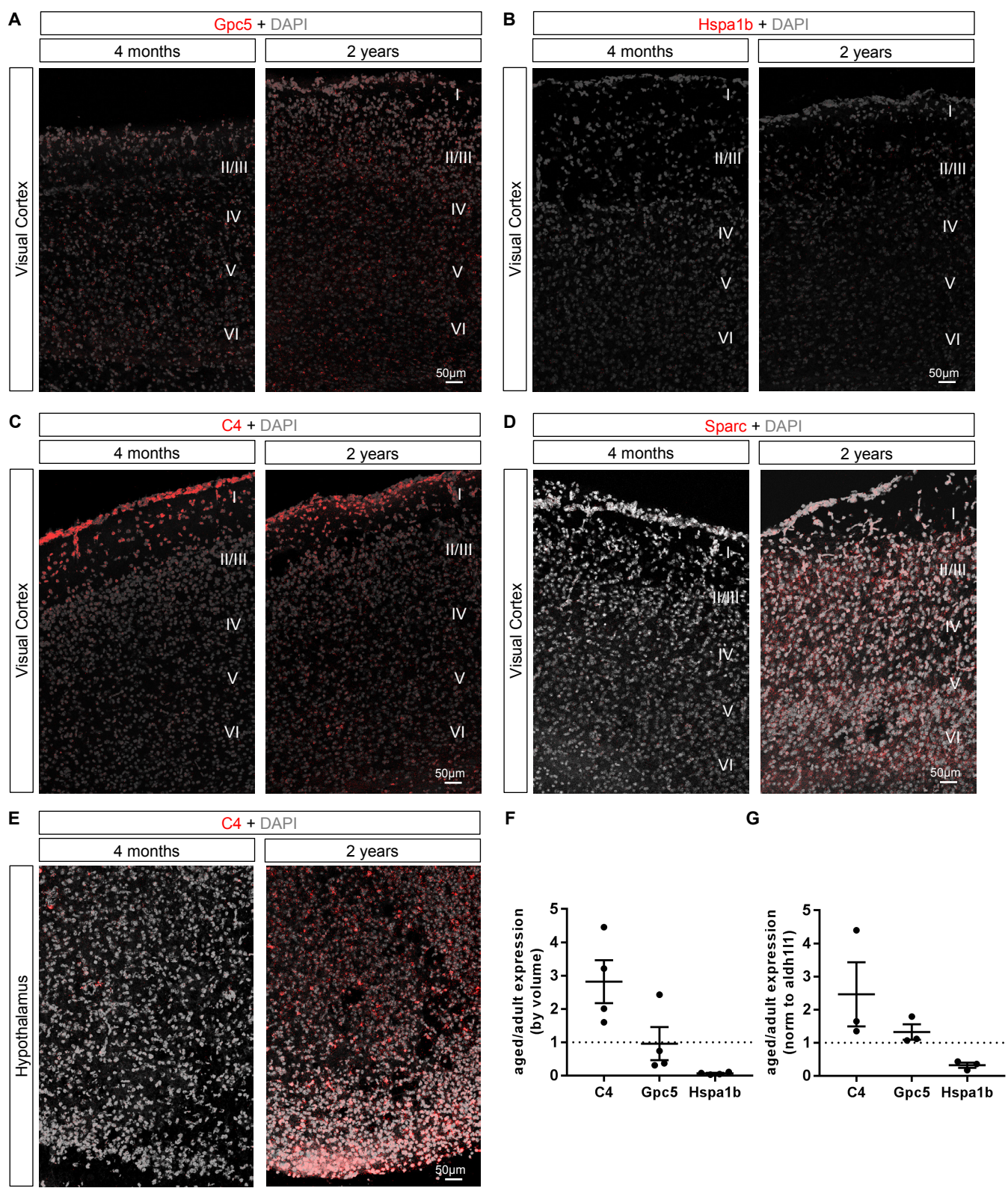

Figure S4, relates to Figure 3. *In situ* hybridization validation of RNAseq changes. *In situ* hybridization to detect mRNA for candidate genes in the VC (**A-D**) and HTH (**E**) of 4 month (left) and 2 year old (right) mouse brain, related to Fig 3 example images. Visual cortex RNAscope for *Gpc5* (**A** unchanged in aging; note same example images as Fig S3), *Hspa1b* (**B,** decreased in aging), *C4* and *Sparc* (**C, D**, increased in aging), and hypothalamic *C4* (**E,** increased in aging). Images are mosaic of tiles acquired at 20x **F,G.** Normalization of *in situ* hybridization data from Fig 3 to either total analyzed volume of stain (**F**) or total intensity of *Aldh1l1* colabel (**G**). The direction of gene expression change matches that in Fig 3.

SUPPLEMENTAL EXPERIMENTAL PROCEDURES

Mice

All mice were maintained in Salk Institute's animal facility in specific pathogen free group housing with ad libitum access to food and water, on a 12 hour light/12 dark cycle.

Astrocyte-ribotag mice were generated by crossing Gfap-cre hemizygous females (B6.Cg-Tg (GFAP-cre)73.12Mvs/J, Jax #012886) to homozygous flox-Rpl22-HA males (B6N.129-Rpl22tm1.1Psam/J, Jax #011029). Male mice heterozygous for flox-Rpl22-HA and hemizygous for cre (astrocyte-ribotag) were used to purify mRNA for astrocyte-enriched RNAseq experiments, at 4 months of age or 2 years of age.

C57Bl6/J wild-type (WT) mice (Jax #000664) were used to validate changes in astrocyte mRNA expression in aging that were detected using RNAseq. For 2-year-old time points, C57bl6/J male 1.5-year-old mice were imported from the National Institutes of Aging and aged for an additional 6 months in the Salk Institute's mouse colony. 4-month-old mice were either bred in-house or purchased from Jackson Laboratories at 10-12 weeks of age and aged to 4 months in Salk animal facilities.

Tissue collection. Mice were anesthetized with an intraperitoneal injection of 100 mg/kg Ketamine (Victor Medical Company)/20 mg/kg Xylazine (Anased) mix in sterile saline before tissue collection, as outlined below.

Ribotag

Brain Dissection Mice were anesthetized between 10am-12pm and transcardially perfused with 10ml PBS then 10ml 1% PFA. The animals were inspected by a veterinarian, and no gross abnormalities or pathology detected. Brains were dissected in (2.5mM HEPES-KOH pH 7.4, 35mM glucose, 4mM NaHCO3 in 1x Hank's Balanced Salt Solution with 100µg/ml cycloheximide added fresh (Heiman et al., 2014). Brains were cut from approximately bregma 2.3 to 1.1 (MC), -0.3 to -1.5 (SC), and at -3.4 (VC), with the cortex then carefully detached from the rest of the brain and any visible white matter removed. Lateral cuts were made 2mm from midline on either side for the MC, at 1.5 and 4mm for SC, and at 1mm and 3mm from the midline for the VC section. For the HTH dissection, a region from the bregma -0.3 to -1.5 slice (SC) was cut ~1.2mm from midline and ~1mm from bottom. The cerebellum was dissected off. All brain regions derive from the same biological replicates to minimize spurious interregional variability, as in (Chai et al., 2017; Morel et al., 2017).These regions were flash frozen in liquid nitrogen, and stored at -80°C until isolation of mRNA.

Ribotag Pulldown A modified Ribotag protocol was performed to isolate astrocyte enriched RNA. Briefly, a dounce homogenizer was used to homogenize brain samples in 2ml cycloheximide-supplemented homogenization buffer (1% NP-40, 0.1M KCl, 0.05M Tris, pH 7.4, 0.012M MgCl2 in RNase free water, with 1:1000 1M DTT, 1mg/mL heparin, 0.1mg/mL cycloheximide, 1:100 Protease inhibitors, and 1:200 RNAsin added fresh). Homogenates were centrifuged and the supernatant incubated on a rotator at 4°C for 4 hours with 5ul anti-HA antibody to bind the HA-tagged ribosomes (CST Rb anti-HA #3724, 1:200). Magnetic IgG beads (Thermo Scientific Pierce #88847) were conjugated to the antibody-ribosome complex via overnight incubation on a rotator at 4°C. Samples were washed with a high salt buffer (0.333M KCl, 1% NP40, 1:2000 1M DTT, 0.1mg/mL cycloheximide, 0.05M Tris pH 7.4, 0.012M MgCl2 in RNase-free water), and RNA released from ribosomes with 350uL RLT buffer (from Qiagen RNeasy kit) with 1% BME. RNA was purified using RNeasy Plus Micro kit (Qiagen 74034) according to manufacturer instructions and eluted into 16ul RNase-free water. Eluted RNA was stored at -80°C. For each brain region/age, 50ul of homogenate (pre- anti-HA antibody addition) was set aside after centrifugation, kept at -20°C overnight, and purified via RNeasy Micro kit as an 'input' sample, and used to determine astrocyte enrichment. RIN values: 4mo_VC_1 (7), 4mo_VC_2 (7), 4mo_VC_3 (6.7), 4mo_SC_1 (8), 4mo_SC_2 (8.2), 4mo_SC_3 (8.2), 4mo_MC_1 (6.5), 4mo_MC_2 (7.3), 4mo_MC_3 (7.3), 4mo_HTH_1 (7), 4mo_HTH_2 (6.5), 4mo_HTH_3 (6.5), 4mo_CB_1 (6.3), 4mo_CB_2 (3.7), 4mo_CB_3 (6.4), 2yo_VC_1 (6.5), 2yo_VC_2 (6), 2yo_VC_3 (6.1), 2yo_MC_1 (5.3), 2yo_MC_2 (7.4), 2yo_MC_3 (6.5), 2yo_HTH_1 (6.3), 2yo_HTH_2 (6.1), 2yo_HTH_3 (5.9), 2yo_CB_1 (4.1), 2yo_CB_2 (5.1), 2yo_CB_3 (4.4), 4mo_VC_1_IN (8), 4mo_SC_IN (8.1), 4mo_MC_1_IN (7.9), 4mo_HTH_1_IN (6.5), 4mo_CB_1_IN (8), 2yo_VC_1_IN (6.7), 2yo_MC_1_IN (6.4), 2yo_HTH_2_IN (6.1), 2yo_CB_1_IN (6.2).

Analysis

Generation of cell type specific gene lists Gene lists were developed from purified cell type RNAseq data from the developing brain (Zhang et al., 2014), selecting genes enriched >10-fold in a given cell type over all other cell types (except for OPCs, which are enriched >10 over all other cell types except newly formed oligodendrocytes), and expressed with FPKM>5 in our input samples. These gene lists were cross-referenced with microarray data from FACS-purified adolescent mouse astrocytes (Cahoy et al., 2008). To ensure astrocyte specificity we excluded any

putative astrocyte marker gene from the Zhang list that showed <2.5-fold enrichment in astrocytes over whole forebrain in the Cahoy list, and excluded putative non-astrocyte cell type markers from the Zhang list that had an expression level >0.25-fold in astrocytes over whole forebrain in the Cahoy list. Genes absent from the Cahoy et al data were excluded. This gave 102 astrocytic genes, 92 neuronal genes, 16 oligodendrocyte precursor cell genes, 26 myelinating oligodendrocyte genes, 33 microglial genes and 30 endothelial genes (Table S1).
Gene ontology annotation was performed using PANTHER version 12 (Mi et al., 2017) using input data as described for Table S5 (genes with >50% change between adult and aged, FPKM of >0.5, expressed at least 0.75-fold of input).
Cutoffs and comparisons Gene lists in supplementary tables were generated as follows.
Table S3 - all changes in aging: genes with an adjusted p<0.05.
Table S4 - astrocyte-expressed changes in aging: genes from S3 with an adjusted p<0.05, FPKM >1, expressed at least 0.75-fold of input.
Table S5 - aging pathway analysis: genes with >50% change between adult and aged, FPKM of >0.5, expressed at least 0.75-fold of input.
Table S6 – inter-regional comparisons all changes: genes with an adjusted p<0.05.
For intra-cortical comparisons each cortical region was compared to the remaining two cortical regions combined, using batch correction in EdgeR to account for sample non-independence within cortical samples.
For cerebellum and hypothalamus comparisons, CB or HTH were compared against combined cortical samples (MC, SC, VC) using batch correction in EdgeR to account for sample non-independence within cortical samples.
Table S7 – astrocyte-enriched inter-regional comparisons: genes from S6 with an adjusted p<0.05, FPKM >1, expressed at least 3-fold of input.
Table S8 - regional pathway analysis: genes with an adjusted p<0.05, FPKM of >1, expressed at least 0.75-fold of input.
Data presentation For gene clustering heatmaps (Figs 2B and 6C), FPKM with a pseudocount of 5 added were used (to decrease the effect of noise of low-expressed genes), and filtered to exclude genes that did not have at least one value >32. These remaining genes (4,401 for aging heatmap, 3,487 for regional comparisons) were log-transformed and clustered using a hierarchical clustering approach: genes were row-scaled and normalized (z-normalized), 1-correlation was used as a distance measure, and the modified Ward's clustering algorithm (part of the R hclust package) was used. Heatmaps were visualized using R version 3.3.2.
Graphs were made with Prism 7 (Graphpad), including scatter plots and heatmaps. InteractiVenn was used to generate Venn diagrams in Figure 2 (Heberle et al., 2015).
Figure 2 - cell-type enrichment, comparing astrocyte-ribotag pulldown to whole brain input. Log2 (fold change) FPKM values averaged from groups of (pulldown FPKM/input FPKM) values from cell-specific genes (Table S1).
Figure 6 - inter-cortical astrocyte comparisons, heatmaps are derived from row z-scores [(ROI FPKM-row mean FPKM)/row standard deviation].
All other heatmaps are based upon log2 (fold change) FPKM values.

Ribotag characterization: Immunohistochemistry
Tissue collection 4-month-old astrocyte-ribotag mice were transcardially perfused with 10ml PBS then 10ml chilled 4% PFA, brains extracted, sagittally cut down the midline, and kept 2 hours to overnight in 4% PFA at 4°C, washed with PBS and placed in 30% sucrose at 4°C until brains sank (24-48 hours). Brains were then embedded in tissue freezing medium (General Data Healthcare TFM-5) and flash frozen in dry ice/95% ethanol, then stored at -80°C.
Sectioning and staining Sagittal brain sections were cut on a cryostat (Hacker Industries OTF5000) onto Superfrost Plus slides (Thermo Scientific 4951PLUS4). Brains were sliced at 25µm and dried at 4°C before staining. For immunofluorescent staining, a hydrophobic barrier was drawn around the sections with a paraffin pen, and blocking solution applied onto the slide (5% heat inactivated normal goat serum (NGS), 100 mM L-lysine, 0.2% triton in PBS) and incubated at room temperature for 1 hour. Slides were incubated overnight with primary antibody in 2.5% NGS, 100 mM L-lysine in PBS, then washed 3 x 5 minutes in 0.2% Triton/PBS, then secondary antibody applied at 1:500 dilution (in 2.5% NGS, 100 mM L-lysine, in PBS) and incubated, covered, for 2 hours at room temperature. For experiments with antibodies raised in goat, bovine serum albumin (BSA) was used instead of NGS with 3% BSA in blocking, and 1% in antibody buffers. Slides were then washed 3 x 5 minutes in 0.2% Triton/PBS, and mounted with Slowfade Gold mounting medium with DAPI (ThermoFisher S36939) with 1.5 glass coverslip (ThermoFisher #12544E), sealed with clear nail polish, and dried in the dark for 30 minutes to 1 hour.
Antibodies Astrocyte/ependymal cells: Rb anti-S100b (Abcam ab52642, 1:500 dilution); OPCs: Rb anti-Ng2 (Millipore Ab532,0 1:200); Oligodendrocytes: Ms anti-APC (Calbiochem Op80, 1:50), Microglia: Rb anti-Iba1 (Wako 016-20001, 1:250), Ependymal: Gt anti-Vimentin (Millipore AB1620, 1:150); Neuron: Ms anti-NeuN

(Millipore MAB377, 1:100), Ribotag marker: Rb anti-HA-tag (CST 3724, 1:500); Ribotag marker: Rt anti-HA-tag (Roche 11867423001, 1:100); Rt secondary Ab w/Alexa 488: (Gt anti-Rat IgG, (Molecular Probes A11006, 1:500); Rt secondary Ab w/Alexa 594: (Gt anti-Rat IgG, (Molecular Probes A11007 1:500); Gt secondary Ab w/Alexa 488: (Dk anti-Goat IgG (Molecular Probes A11055 1:500); Ms secondary Ab w/Alexa 488: (Gt anti-Mouse IgG (Molecular Probes A11029 1:500); Ms secondary Ab w/Alexa 594: (Gt anti-Mouse IgG (Molecular Probes A11032 1:500); Rb secondary Ab w/Alexa 488: (Gt anti-Rabbit IgG (Molecular Probes A11034 1:500); Rb secondary Ab w/Alexa 594: (Gt anti-Rabbit IgG (Molecular Probes A11037 1:500); Rb secondary Ab w/Alexa 594: (Dk anti-Rabbit IgG (Molecular Probes A21207 1:500).

Imaging 3 x 16-bit images per brain (from different brain sections – technical replicates), from 3 brains (biological replicates), of 500x500µm of the visual cortex, motor cortex, hypothalamus, and cerebellum were acquired with an AxioImager.Z2 with Apotome.2 module and AxioCam HR3 camera (Zeiss). To image a whole region, multiple tiled images were taken with 10% overlap using the mosaic function, and stitched in Axiovision (Zeiss). A Plan-Apochromatic 20x objective (NA 0.8) was used with 0.37x0.37µm pixel scaling for cell-type specific stains. A Plan-Apochromatic 10x objective (NA 0.45) was used for a whole brain overview of HA stain.

Analysis FIJI (Schindelin et al., 2012) was used to determine the number of ribotag positive cells and their overlap with cell-specific staining. Thresholding was performed on the ribotag labeled image (stained with an anti-HA tag antibody) and the 'Analyze Particles' function was used with a minimum area of 20-40µm to automatically separate and quantify the total number of ribotag positive cells. The number of double-labeled ribotag and cell type antibody positive cells were manually counted. This generated the proportion of ribotag positive cells that also label for the cell-specific marker.

Ribotag characterization*: qRT-PCR*

To confirm cell-type specificity, RNA from the hypothalamus and cerebellum of 2 year old astrocyte-ribotag pulldowns was compared to RNA isolated from the whole homogenate (input). cDNA was synthesized via rtPCR from 50-100ng of RNA using Superscript VILO master mix (Thermo Fisher Scientific 11755050) according to manufacturer instructions. 2µl of the obtained cDNA was used for qPCR reaction, performed with SYBR green PCR mastermix (ThermoFisher 4309155) (run with a standard protocol on an Applied Biosystems 7300). All samples were run with 3 biological replicates, each consisting of 3 technical replicates. All primers from Integrated DNA Technologies. For analysis, samples were normalized to a housekeeping gene (Gapdh) run in the same qPCR plate with cDNA from the same dilution, and compared to input samples from the same experiment run in the same plate.

Primers used:

Aldhl1l1 (astrocyte, for: CATATTTGCTGACTGCGACCTC; rev: TTCACACCACGTTGGCAATAC);
Gfap (astrocyte, for: TACCAGGAGGCACTTGCTCG; rev: CCACAGTCTTTACCACGATGTTCC);
Syt1 (neuron, for: CTGCATCACAACACTACTAGC; rev: CCAACATTTCTACGAGACACAG);
Psd95 (neuron, for: GTGGGCGGCGAGGATGGTGAA; rev: CCGCCGTTTGCTGGGAATGAA);
Camk2 (neuron, for: AATGGCAGATCGTCCACTTC; rev: ATGAGAGGTGCCCTCAACAC);
Mobp (oligo, for: TCTTCCTCCTGTTCCCTCTCTTG; rev: GGATTTACATTAGGCAAAGCATTGG);
Mbp (oligo, for: GGCAAGGTACCCTGGCTAAA; rev: GTTTTCATCTTGGGTCCGGC);
Gapdh (housekeeping, for: TGCCACTCAGAAGACTGTGG; rev: GCATGTCAGATCCACAATGG)

GFAP immunohistochemistry

Tissue collection 2-year-old and 4-month-old C57Bl6/J mice were transcardially perfused with PBS, brains extracted and cut down the midline, embedded in OCT (Scigen #4583), flash-frozen in a 95% ethanol/dry ice bath and kept at -80°C, as outlined above.

Gfap staining 4 x 4-month-old and 4 x 2-year-old brains were sectioned on a cryostat at 20µm (as above), sections stored at -20C, and fixed in 4% PFA for 8 minutes at 4°C, followed by 3 washes in PBS. From there, immunohistochemistry was performed as outlined above with Rb anti-GFAP primary antibody (Abcam ab7260, 1:500 dilution) and Alexa 594-conjugated secondary antibody (Gt anti-Rabbit IgG, Molecular Probes A11037, 1:500).

Imaging 3 x 16-bit tiled images per brain (from different sections – technical replicates), from 4 brains (biological replicates), of hypothalamus and visual cortex per animal were taken of 500µm x 500µm, consisting of 3 x 1.5µm sections in the z-dimension. A Zeiss LSM700 confocal with a Plan-Apochromatic 20x objective (NA 0.8) and AxioObserver camera was used to take images with 0.17x0.17x1.5µm pixel scaling. Identical imaging conditions (laser power, gain) were used for 4-month and 2-year-old samples. The whole brain overview images were acquired using set exposure with an AxioImager.Z2 with a Plan-Apochromatic 10x objective (NA 0.45) and AxioCam HR3 camera (Zeiss) at 0.645x0.645µm pixel scaling.

GFAP analysis For confocal sections, a maximum intensity projection was made from all 3 z-planes, and total fluorescence intensity was quantified using the ImageJ measure function, excluding meninges and pia. Analysis was also performed excluding GFAP around blood vessels, with no difference in outcome.

***In situ* hybridization**

Tissue collection and processing was carried out as described for GFAP staining, and brains were sagittally sectioned at 16-20µm. To perform the *in situs,* RNAscope 2.5 HD multiplex fluorescent Manual Assay kit (ACDbio #320850) was used with modifications - a 25-30 minute permeabilization step using Protease IV (ACDbio #322340) and a final 5 minute DAPI incubation step used to visualize nuclei (1:1000 dilution in PBS; Millipore #5.08741.0001). The primary probe of interest was detected with the Atto-550 detection reagent, with the secondary probe of interest detected using Atto-647 (except for the SPARC experiment, where SPARC was detected with Atto-550, and the secondary probe with Alexa-488).

Probes Serpina3n (Cat #430199 target; NM_009252.2, 745-2005bp); Sparc (#466781-C2; target NM_009242.5, 337-1185bp); Gpc5 (#442831; target NM_175500.4, 389-1414bp); Hspa1b (#488351; target NM_010478.2, 2162-2790bp); C4 (#445161; NM_009780.2, 1644-2631bp); Aldh1l1 (#405891-C2; target NM_027406.1, 1256-2112bp); Aldh1l1 (#405891, target NM_027406.1, 1256-2112); DapB (negative ctrl; #320751, target EF191515, 414-862bp)

Imaging 3 x 16-bit tiled images per region (each from a different brain slice – technical replicates) from 4 brains per age (biological replicates) of at least 500x500µm, with 3 x 1.5µm sections in the z-dimension were obtained. A Zeiss LSM700 confocal with a Plan-Apochromatic 20x objective (NA 0.8) was used to take images with 0.17x0.17x1.5µm pixel scaling. In addition to DAPI, primary probe and secondary probe channels, a blank (unstained) channel was imaged in the 488 wavelength (except for SPARC, whose blank channel was imaged at 647) in order to image auto fluorescent lipofuscin to aid in image analysis (see below). For all experiments, imaging parameters were kept constant between 4-month and 2-year-old samples.

Analysis Analysis of the fluorescent probe signal was hindered in the 2-year old brain due to the high presence of autofluorescent lipofuscin in the aged tissue, which was present in all channels. To eliminate this from the channels containing probe to enable analysis, images were analyzed in Imaris (Bitplane). A 3-dimensional mask from the blank channel (where only lipofuscin fluoresced - see Fig S3) was constructed using the 'surfaces' function using an absolute intensity threshold and size filters. This mask was then subtracted from the channels containing probe, to create an image that just contained signal from the probe. The surface function was then used on this masked channel to define the probe staining area. Total intensity of fluorescence of probe staining, and area of staining, were then quantified with the Imaris 'statistics' function and normalized to tissue volume. Meninges and pia were excluded from analysis. The intensity measure is reported as the ratio of 2-year-old/4-month-old in the figures; the same trends in expression are seen when total area is used for analysis. In order to ensure that the effect seen is not a consequence of altered tissue quality with age, total probe intensity of a given sample was normalized to the total probe intensity of a second *in situ* probe within the same tissue section, Aldh1l1 to mark astrocytes. Second-probe normalized values for a given primary probe exhibit the same trend as non-normalized data.

Graphs and statistics

Graphs were made with Prism 7 (Graphpad), including scatter plots and heatmaps. Statistics were performed as outlined in the RNAseq section.

SUPPLEMENTAL REFERENCES

Cahoy, J.D., Emery, B., Kaushal, A., Foo, L.C., Zamanian, J.L., Christopherson, K.S., Xing, Y., Lubischer, J.L., Krieg, P.A., Krupenko, S.A., *et al.* (2008). A transcriptome database for astrocytes, neurons, and oligodendrocytes: a new resource for understanding brain development and function. J Neurosci 28, 264-278.

Chai, H., Diaz-Castro, B., Shigetomi, E., Monte, E., Octeau, J.C., Yu, X., Cohn, W., Rajendran, P.S., Vondriska, T.M., Whitelegge, J.P., *et al.* (2017). Neural Circuit-Specialized Astrocytes: Transcriptomic, Proteomic, Morphological, and Functional Evidence. Neuron 95, 531-549.e539.

Doyle, J.P., Dougherty, J.D., Heiman, M., Schmidt, E.F., Stevens, T.R., Ma, G., Bupp, S., Shrestha, P., Shah, R.D., Doughty, M.L., et al. (2008). Application of a Translational Profiling Approach for the Comparative Analysis of CNS Cell Types. Cell 135, 749-762.

Heberle, H., Meirelles, G.V., da Silva, F.R., Telles, G.P., and Minghim, R. (2015). InteractiVenn: a web-based tool for the analysis of sets through Venn diagrams. BMC Bioinformatics 16, 169.

Heiman, M., Kulicke, R., Fenster, R.J., Greengard, P., and Heintz, N. (2014). Cell type–specific mRNA purification by translating ribosome affinity purification (TRAP). Nat Protocols 9, 1282-1291.

Mi, H., Huang, X., Muruganujan, A., Tang, H., Mills, C., Kang, D., and Thomas, P.D. (2017). PANTHER version 11: expanded annotation data from Gene Ontology and Reactome pathways, and data analysis tool enhancements. Nucleic Acids Research 45, D183-D189.

Morel, L., Chiang, M.S.R., Higashimori, H., Shoneye, T., Iyer, L.K., Yelick, J., Tai, A., and Yang, Y. (2017). Molecular and Functional Properties of Regional Astrocytes in the Adult Brain. The Journal of Neuroscience 37, 8706-8717.

Schindelin, J., Arganda-Carreras, I., Frise, E., Kaynig, V., Longair, M., Pietzsch, T., Preibisch, S., Rueden, C., Saalfeld, S., Schmid, B., *et al.* (2012). Fiji: an open-source platform for biological-image analysis. Nat Meth 9, 676-682.

Zhang, Y., Chen, K., Sloan, S.A., Bennett, M.L., Scholze, A.R., O'Keeffe, S., Phatnani, H.P., Guarnieri, P., Caneda, C., Ruderisch, N., *et al.* (2014). An RNA-Sequencing Transcriptome and Splicing Database of Glia, Neurons, and Vascular Cells of the Cerebral Cortex. J Neurosci 34, 11929-11947.